mined as translational repression of target genes, such as *m-Numb*, a negative regulator of Notch signaling.[10] In both mice and humans, Msi-1 has been shown to be expressed in ISCs, but in sharp contrast, its expression is completely lacking in mature Paneth cells.[8,9,11] Thus, Msi-1 might function within intestinal epithelial cells (IECs) to maintain their undifferentiated state.[12,13] However, the molecular function of Msi-1 in IECs has never been described.

Herein, we show that expression of Msi-1 in IECs suppressed expression of Paneth cell-specific genes, such as *PLA2G2A*. Msi-1 appeared to downregulate expression of the *PLA2G2A* gene at the mRNA level, through a molecular pathway independent of both Notch and Wnt, the two major molecular pathways that are known to regulate Paneth cell differentiation. These results suggest that Msi-1 is a negative regulator of Paneth cell differentiation in IECs, and that it has a functional role in maintaining the undifferentiated state of ISCs.

Materials and methods

Cell culture

Human colon cancer-derived LS174T cells were cultured in minimal essential medium (GIBCO, Billings, MT, USA) supplemented with 10% fetal bovine serum, 2 mM L-glutamine, 100 U/ml penicillin, and 100 mg/ml streptomycin (Invitrogen, Carlsbad, CA, USA), at 37°C in a humidified incubator with 5% CO_2.

Plasmids

For construction of the expression plasmid for Msi-1 (pcDNA3.0-Msi-1), the entire coding lesion of the mouse *Msi-1* gene was polymerase chain reaction (PCR) amplified from pcDNA3.0-FLAG-Msi-1 (kindly provided by Dr. Hideyuki Okano), and inserted into pcDNA3.0 (Invitrogen). For construction of the enhanced green fluorescent protein (EGFP) expression plasmid (pCMV-FLAG-EGFP), the coding sequence of pEGFP-C1 (Stratagene, La Jolla, CA, USA) was PCR amplified and inserted into the pCMV-FLAG-Tag vector (Stratagene).

Establishment of cell lines stably expressing Msi-1 or EGFP

Expression plasmids for Msi-1 (pcDNA3.0-Msi-1) or EGFP (pCMV-FLAG-EGFP) were transfected into LS174T cells as previously described.[14] After 2 days of culture, cells were selected by addition of G418 (1 mg/ml) to the culture medium. Subsequently, G418-resistant cells were cloned into sublines expressing Msi-1 or EGFP, designated as LS174T/Msi-1 cells or LS174T/GFP cells, respectively.

Microscopic imaging and immunostaining of cultured cells

Microscopic images of cultured cells were collected using an epifluorescence microscope system (BZ-2000, Keyence, Osaka, Japan). Immunostaining of cultured cells were done as previously described.[15,16] For detection of Musashi-1, primary antibody (14H1, kindly provided by Dr. Hideyuki Okano) was diluted to 1:1000 and detected by an Alexa-488-conjugated secondary antibody (Molecular Probes, Eugene, OR USA). Cells were counterstained by 4′,6-diamino-2-phenylindole (DAPI), and mounted in Vectashield mounting medium (Vector Laboratories, Burlingame, CA, USA).

Cell proliferation assay

Incorporation of bromodeoxyuridine (Brd-U) was examined using a cell proliferation enzyme-linked immunosorbent assay (ELISA) kit (Roche Diagnostics, Mannheim, Germany), according to the manufacturer's instructions. Briefly, cells were seeded onto a 96-well dish at various cell densities, cultured for 48 h, and labeled with Brd-U for 8 h at the end of culture. Each condition was measured in triplicate and the results analyzed by Student's *t* test.

Reverse transcription-polymerase chain reaction

Total RNA was prepared using TRIzol reagent (Invitrogen) according to the manufacturer's instructions. Reverse transcription (RT) was carried out as previously described.[15] Forward and reverse primers used for the PCR reaction are summarized in Table 1. For semiquantitative PCR, 1 µl of cDNA was amplified with 0.25 U of LA *Taq* polymerase (Takara, Otsu, Japan), using the optimized amplification cycles determined for each primer set. Amplified products were separated by 1.8% agarose gel electrophoresis, stained with ethidium bromide, and visualized by the Lumi-Imager F1 system (Roche Diagnostics). For quantitative PCR, 1 µl of cDNA was amplified using SYBR green master mix (Qiagen, Valencia, CA, USA), and analyzed by a 7500 real-time PCR system (Applied Biosystems, Foster City, CA, USA).

Immunoblotting

Immunoblot analysis was done as previously described.[15] Briefly, 1×10^6 cells were seeded onto 6-cm culture dishes and collected for protein extraction after 48 h of

Table 1. Primers used in the present study

Gene	Primer sequence	
	Forward	Reverse
Musashi-1	5′-GGCTTCGTCACTTTCATGGACCAGGCG-3′	5′-GGGAACTGGTAGGTGTAAC-3′
MUC2	5′-CTGCACCAAGACCGTCCTCATG-3′	5′-GCAAGGACTGAACAAAGACTCAGAC-3′
TFF3	5′-TGAGGAGTACGTGGGCCTGTCTGCAAA-3′	5′-CGGGTGGAGCATGGGACCTTTATT-3′
KLF-4	5′-GGGAGAAGACACTGCGTCA-3′	5′-GGAAGCACTGGGGGAAGT-3′
Isomaltase	5′-TACTAGAAGACAAGATCCCGCT-3′	5′-GTAGTTCCTTTCCCCCATACAT-3′
Lactase	5′-CCCCAAAGCATCAGCGAAGTT-3′	5′- CTACACGTTTCCGCAAGAGCT-3′
PLA2G2A	5′-ACCATGAAGACCCTCCTACTG-3′	5′-GAAGAGGGGACTCAGCAACG-3′
HD-5	5′-CCCAGCCATGAGGACCATCG-3′	5′-TCTATCTAGGAAGCTCAGCG-3′
HD-6	5′-CCACTCCAAGCTGAGGATGATC-3′	5′-CCACTCCAAGCTGAGGATGATC-3′
Lysozyme	5′-CTCTCATTGTTCTGGGGC-3′	5′-ACGGACAACCCTCTTTGC-3′
c-Myc	5′-CTTCTGCTGGAGGCCACAGCAAACCTCCTC-3′	5′-CCAACTCCGGGATCTGGTCACGCAGGG-3′
EphB3	5′-AGCAACCTGGTCTGCAAAGT-3′	5′-TCCATAGCTCATGACCTCCC-3′
G3PDH	5′-TGAAGGTCGGAGTCAACGGATTTGGT-3′	5′-CATGTGGGCCATGAGGTCCACCAC-3′
GFP	5′-TGAAGGTCGGAGTCAACGGATTTGGT-3′	5′-CATGTGGGCCATGAGGTCCACCAC-3′

culture. Total cell lysate was prepared using radioimmunoprecipitation assay buffer. Fifty micrograms of each lysate was subjected to analysis. Primary antibodies used were as follows: mouse anti-Musashi-1 (1:500, Chemicon, Temecula, CA, USA), rabbit anti-GFP (1:2500, MBL, Nagoya, Japan), Goat anti-NUMB (1:100, Santa Cruz Biotechnology, Santa Cruz, CA, USA), rabbit anti-Hes1 (kindly provided by Dr. T. Sudo), mouse anti-β-actin (1:5000, Sigma, St. Louis, MO, USA). Primary antibodies were detected by the appropriate horseradish peroxidase-conjugated secondary antibodies, and visualized by the Lumi-Imager F1 system (Roche Diagnostics) using enhanced chemiluminescence (Amersham Biosciences, Buckinghamshire, UK) as a substrate.

Quantification of PLA2G2A secretion

For PLA2G2A protein quantification, 1×10^6 cells were seeded onto a 6-cm dish and cultured for up to 5 days. Supernatants were collected at 1, 3, and 5 days of culture and analyzed with a sPLA2 (human type IIA) enzyme immunoassay (EIA) kit (Cayman Chemical, Ann Arbor, MI, USA). The assay was performed in triplicate, and the results statistically analyzed by paired Student's *t* test.

Reporter assays

Reporter assays using the dual luciferase system (Promega, Madison, WI, USA) has been previously described.[15] TOP-Flash and FOP-Flash reporter plasmids were purchased from Upstate Biotechnology (Lake Placid, NY, USA). Each condition was examined in triplicate and the results analyzed by Student's *t* test.

Human intestinal tissue specimens

Normal human small intestinal tissues were obtained from patients who underwent surgery for the treatment of Crohn's disease at Yokohama Municipal General Hospital, and macroscopically intact regions of each specimen were subjected for immunohistochemical staining. Written informed consent was obtained from each patient, and the study was approved by the ethics committee of Yokohama Municipal General Hospital and Tokyo Medical and Dental University.

Immunohistochemistry

Immunohistochemistry using human intestinal tissues has been previously described.[11] Primary antibodies used were as follows: Rat anti-Musashi-1 (1:1000, kindly provided by Dr. Hideyuki Okano), and Goat-anti-human PLA2G2A (1:200, sc-14468, Santa Cruz Biotechnology). Microwave treatment (500 W, 10 min) in 10 mM citrate buffer was required for detection of both Msi-1 and PLA2G2A. Msi-1 antibody was visualized using Alexa-488-conjugated Tyramide (Molecular Probes) as a substrate for the avidin–biotin complex (Vector Laboratories), whereas PLA2G2A antibody was visualized by Alexa-594-conjugated secondary antibody (Molecular Probes). Sections were counterstained with DAPI and mounted in Vectashield mounting medium (Vector Laboratories). Fluorescent images were captured by the epifluorescence microscope system (BZ-2000, Keyence).

Results

Establishment of stable cell lines constitutively expressing Msi-1

To analyze the functional role of Msi-1, we planned to assess the effect of Msi-1 expression in human IECs. For this purpose, we employed LS174T cells as the parental (host) cells, as we have previously shown that these cells readily express a wide variety of lineage-specific genes,[15,16] but do not express detectable amount of endogenous Msi-1 protein (Fig. 1B). These features of LS174T cells makes them an ideal model for examining whether expression of Msi-1 can modulate proliferation as well as differentiation of human IECs. Following transfection of an expression plasmid for Msi-1, we successfully generated three clones of LS174T cells that stably expressed Msi-1 (designated hereafter as LS174T/Msi-1 cells). We also generated another clone of LS174T cells that stably expressed EGFP to serve as a control (LS174T/GFP cells). RT-PCR analysis of these generated cell clones revealed mRNA expression from the corresponding transgenes (Fig. 1A). Also, immunoblot analysis clearly showed expression of green fluorescent protein (GFP) or Msi-1 protein in LS174T/GFP or LS174T/Msi-1 cells, respectively (Fig. 1B). An epifluorescence view of these cells also assured constitutive expression of GFP in all of the LS174T/GFP cells but not in the other cell clones (Fig. 1C). In contrast, immunostaining of Msi-1 protein revealed constitutive expression of Msi-1 protein in all of the LS174T/Msi-1 cells but not in the other cell clones (Fig. 1D). A phase-contrast view showed no clear difference between parental cells and LS174T/GFP cells, as both cell clones aggregated to form a round cell colony consisting of vertically piled-up cells (Fig. 1C). LS174T/Msi-1 cells, however, failed to form such cell colonies, but showed a very flat cell morphology and appeared to spread horizontally as a monolayer of cells (Fig. 1C). These results collectively confirmed that the generated cells surely expressed GFP or Msi-1 protein in a constitutive manner, and also suggested that expression of Msi-1 might have induced some intracellular changes influencing the shape and nature of colony formation of LS174T cells.

Expression of Msi-1 did not change cell proliferation but decreased expression of Paneth cell-specific genes in LS174T cells

As we found morphological changes in cells and colony shape of LS174T/Msi-1 cells (Fig. 1C), we examined whether they underwent changes in cell proliferation. Analysis of Brd-U incorporation, however, showed no significant change in LS174T/Msi-1 cells compared with LS174T/GFP cells (Fig. 2A). Next, we analyzed the expression of lineage-specific genes, to evaluate the effect of Msi-1 expression upon IEC differentiation. Results of the RT-PCR analysis showed no change in expression of goblet cell-specific genes such as *MUC-2*, *TFF-3*, or *KLF-4* (Fig. 2B). Also, genes specific for absorptive cell lineage (Fig. 2B) or neuroendocrine cell lineage (data not shown) remained undetectable in both LS174T/GFP and LS174T/Msi-1 cells. In sharp contrast, expression of Paneth cell-specific genes such as *PLA2G2A*, *HD-5*, and *Lysozyme*[17] appeared to be decreased in LS174T/Msi-1 cells, compared with LS174T/GFP cells (Fig. 2B). This suggested that expression of Msi-1 might have suppressed expression of Paneth cell-specific genes in LS174T/Msi-1 cells.

To confirm our earlier results, we further examined the expression of one of the Paneth cell-specific genes, *PLA2G2A*, as it showed the clearest decrease in mRNA in LS174T/Msi-1 cells (Fig. 2B). Quantitative RT-PCR confirmed an up to 90% decrease of *PLA2G2A* mRNA expression in LS174T/Msi-1 cells, compared with LS174T/GFP cells (Fig. 3A). PLA2G2A protein secretion also showed a significant decrease in LS174T/Msi-1 cells compared with LS174T/GFP cells (Fig. 3B). From these results, Msi-1 appeared to suppress *PLA2G2A* gene expression at the mRNA level, leading to decreased secretion of mature PLA2G2A protein.

Expression of Msi-1 did not change the expression level of genes downstream of Notch and Wnt pathways in LS174T cells

As it is has been previously reported that one of the molecular functions of Msi-1 is translational repression of m-Numb, a negative regulator of Notch signaling,[10] we next examined whether suppression of *PLA2G2A* gene expression might be induced through modulation of the Notch signaling pathway. Immunoblot analysis of m-Numb or Hes1 expression, however, showed equivalent expression of both proteins in LS174T/Msi-1 and LS174T/GFP cells (Fig. 4A). Consistently, the reporter assay for RBP-Jk-dependent transcription showed no significant difference between LS174T/Msi-1 and LS174T/GFP cells (Fig. 4B). These results suggest that expression of Msi-1 had minimal effect upon expression of *m-Numb* or target genes of Notch in LS174T cells.

In addition to Notch, the Wnt signaling pathway has been described as another key signaling pathway for Paneth cell differentiation.[7,18] Also, *PLA2G2A* has been shown to be one of the direct target genes of the canonical Wnt pathway.[19] As a recent study reported that Msi-1 could modulate signaling of the Wnt pathway,[20] we next examined whether expression of Msi-1 had modulated the intracellular activity of the Wnt pathway. Consistent with the previous result in mammary

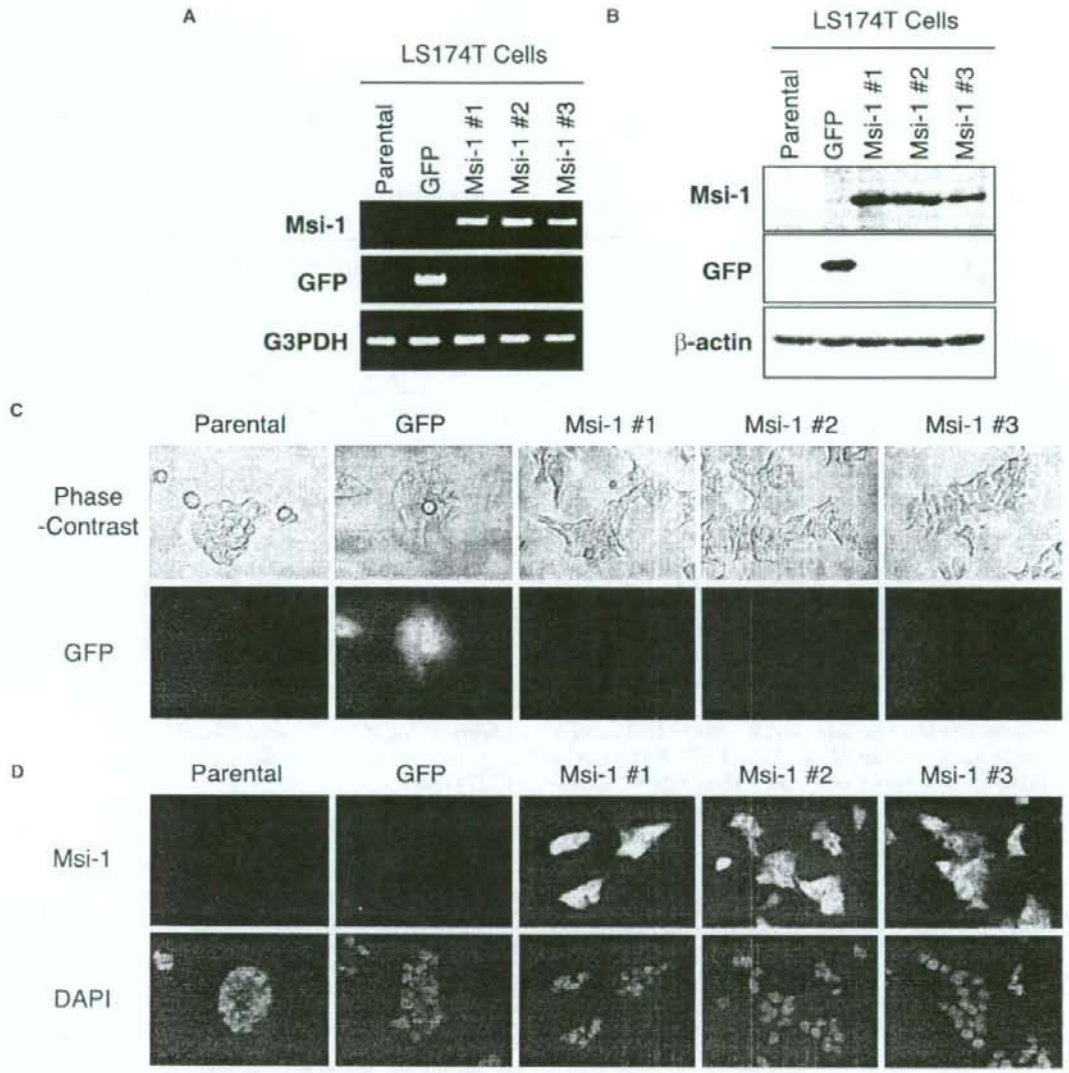

Fig. 1. Establishment of cell lines stably expressing Musashi-1. **A** Reverse transcriptase-polymerase chain reaction (RT-PCR) analysis of the generated cell lines. *GFP* (green fluorescent protein) indicates a clone of LS174T cells that constitutively expresses enhance green fluorescent protein (EGFP) (LS174T/GFP cells), whereas *Msi-1 #1*, *Msi-1 #2*, and *Msi-1 #3* indicate distinct clones of LS174T cell that constitutively express Musashi-1 (Msi-1) (LS174T/Msi-1 cells). *Parental* indicates the parental LS174T cells. Note that mRNA expression of Msi-1 or GFP is clearly observed in LS174T/GFP cells or LS174T/Msi-1 cells, respectively, but not in parental cells. **B** Immunoblot analysis of the generated cell lines. Total cell lysate obtained from each cell line was analyzed for expression of Msi-1, GFP, and β-actin. Msi-1 protein was detected exclusively in the LS174T/Msi-1 cell lines (Msi-1 #1, #2, and #3), whereas GFP protein was detected exclusively in LS174T/GFP cells (GFP). **C** Morphological changes and GFP expression in the generated cell lines. Phase contrast view of the cell lines shows aggregated, round colony formation in parental and LS174T/GFP cells (GFP), whereas a flat, monolayer expansion is observed in LS174T/Msi-1 cells (Msi-1 #1, #2, and #3). An epifluorescence view confirmed stable expression of GFP in LS174T/GFP cells, but not in other cells. **D** Expression of Msi-1 protein in generated cell lines. Cells were stained by Msi-1 specific antibody and visualized by Alexa-488-conjugated secondary antibody. Cells were also counterstained with 4′,6-diamino-2-phenylindole (DAPI). Staining confirmed the expression of Msi-1 protein in LS174T/Msi-1 cells (Msi-1 #1, #2, and #3), and not in other cells

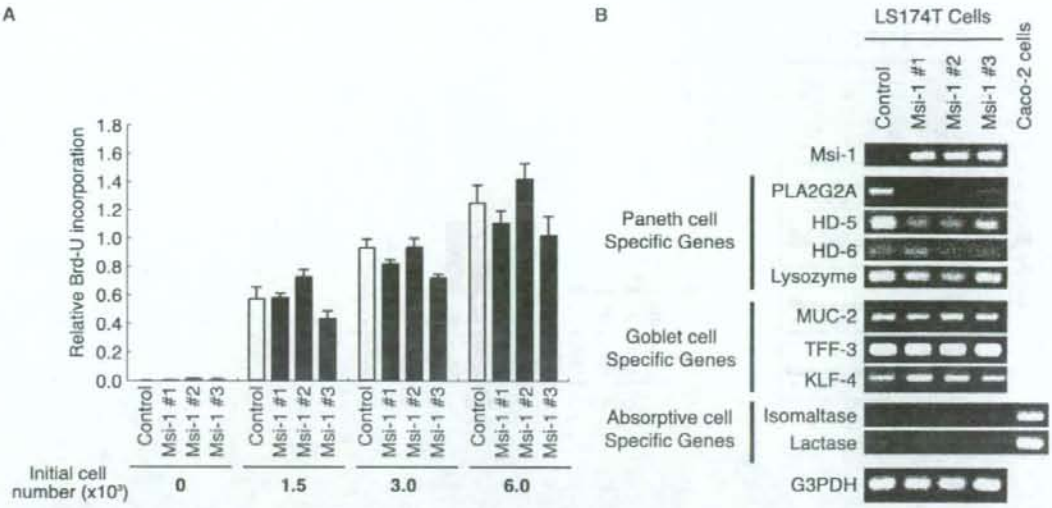

Fig. 2. Expression of Msi-1 does not change cell proliferation, but decreases expression of Paneth cell-specific genes in LS174T cells. **A** Bromodeoxyuridine (*Brd-U*) incorporation of the generated cell lines. Cells were cultured at various densities and subjected to Brd-U incorporation analysis using an enzyme-linked immunosorbent assay. Results of LS174T/GFP cells served as a control. Error bar represents SD. **B** Semiquantitative RT-PCR analysis of lineage-specific genes in the generated cell lines. Total RNA was isolated from LS174T/GFP cells (*Control*) or LS174T/Msi-1 cells (*Msi-1 #1*, *Msi-1 #2*, and *Msi-1 #3*), and subjected to analysis. A corresponding sample prepared from Caco-2 cells served as a positive control for absorptive cell-specific genes. Glyceraldehyde-3-phosphate dehydrogenase (*G3PDH*) served as an internal control

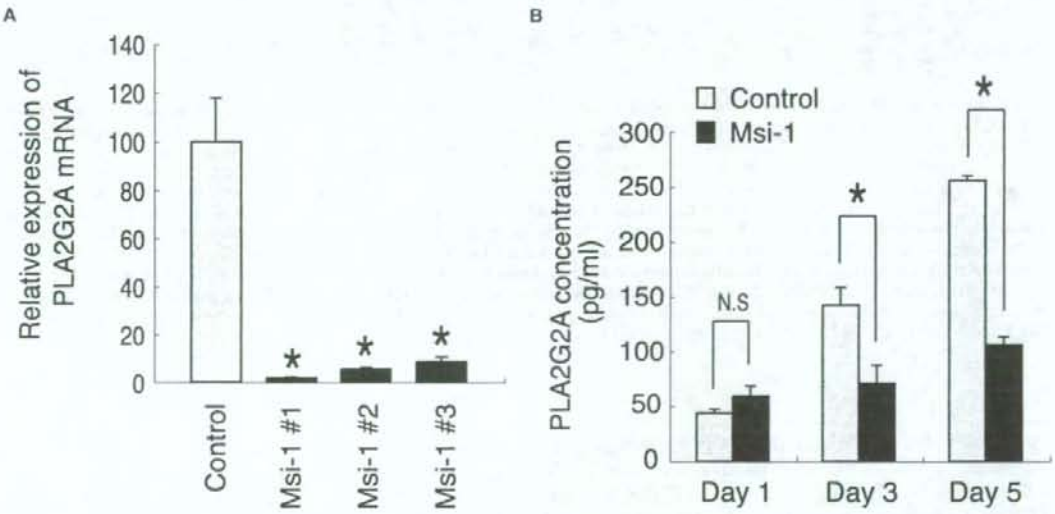

Fig. 3. Expression of Msi-1 suppresses gene expression of *PLA2G2A* in LS174T cells. **A** Quantitative RT-PCR analysis of *PLA2G2A* expression in the generated cell lines. Results of LS174T/GFP cells served as a control. Error bar represents SD. $^*P < 0.05$, Student's *t* test. **B** Analysis of PLA2G2A protein secretion by LS174T parental cells (*Control*) or LS174T/Msi-1 cells (*Msi-1*). Control or LS174T/Msi-1 cells were cultured for up to 5 days, and the amount of secreted PLA2G2A was measured by enzyme immunoassay at different time points. Error bar represents SD. $^*P < 0.05$, Student's *t* test

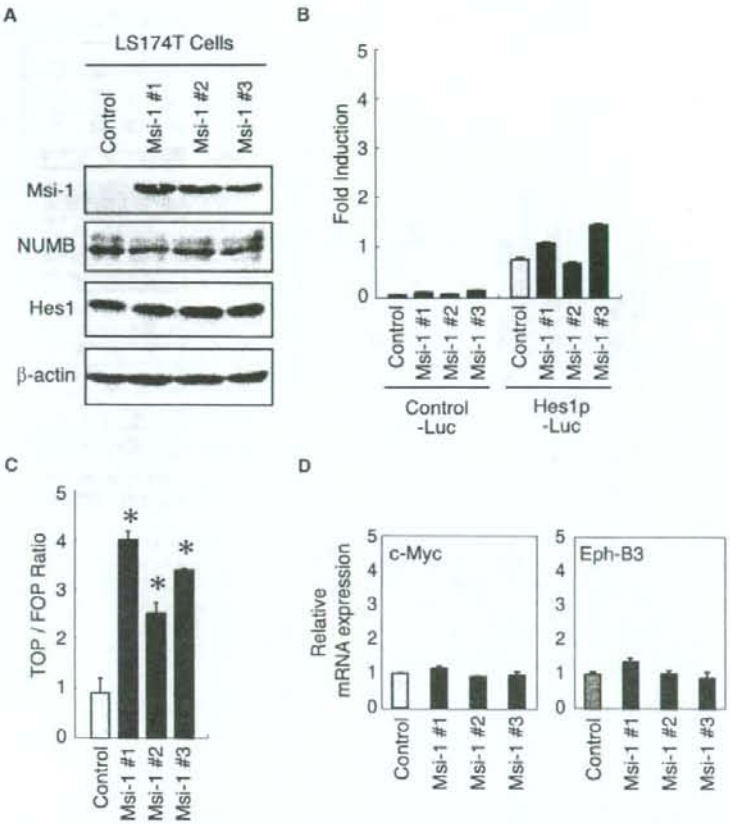

Fig. 4. Expression of Msi-1 has no effect upon expression of target genes downstream of Notch or Wnt pathways in LS174T cells. **A** Immunoblot analysis of Notch pathway genes in the generated cell lines. Total cell extract prepared from LS174T/GFP cells (*Control*) or LS174T/Msi-1 cells (*Msi-1 #1*, *Msi-1 #2*, and *Msi-1 #3*) was subjected to analysis. Result for *m-Numb* shows two distinct bands, one representing the short (*upper band*) and the other the long (*lower band*) isoform of the *m-Numb* gene. **B** Luciferase reporter assay for analysis of RBP-Jk dependent transcriptional activity. Hes1p-Luc contains six tandem repeats of RBP-Jk binding sites, whereas Control-Luc contains only the core promoter element derived from the chicken *β-actin* gene. Each data point was normalized by the corresponding Renilla luciferase activity. Error bar represents SD. **C** Luciferase reporter assay for analysis of TCF-dependent transcriptional activity. Firefly luciferase activity of the TOP-flash or FOP-flash vector was normalized by the corresponding Renilla luciferase activity. Data are shown as ratio of normalized TOP-flash and FOP-flash activity. Error bar represents SD. $*P < 0.05$ compared with control cells, Student's *t* test. **D** Quantitative RT-PCR analysis of Wnt target genes in the generated cell lines. Relative expression level of c-Myc and Eph-B3 are shown. Error bar represents SD. Expression in LS174T/GFP cells (*Control*) is set to 1

epithelial cells,[20] we found that TCF-dependent transcriptional activity was upregulated two- to four fold in LS174T/Msi-1 cells compared with LS174T/GFP cells (Fig. 4C). However, expression of c-Myc and Eph-B3 showed no significant change between LS174T/Msi-1 cells and LS174T/GFP cells (Fig. 4D), suggesting that an additional increase of TCF-dependent transcriptional activity in these cells may not necessarily lead to changes in the expression level of the downstream target genes. These results showed that expression of Msi-1 in LS174T cells has only a minimal effect upon Notch or Wnt target genes, and suggested that changes observed in LS174T/Msi-1 cells, such as cell morphology or *PLA2G2A* expression, are presumably mediated through a mechanism independent of such molecular signaling pathways.

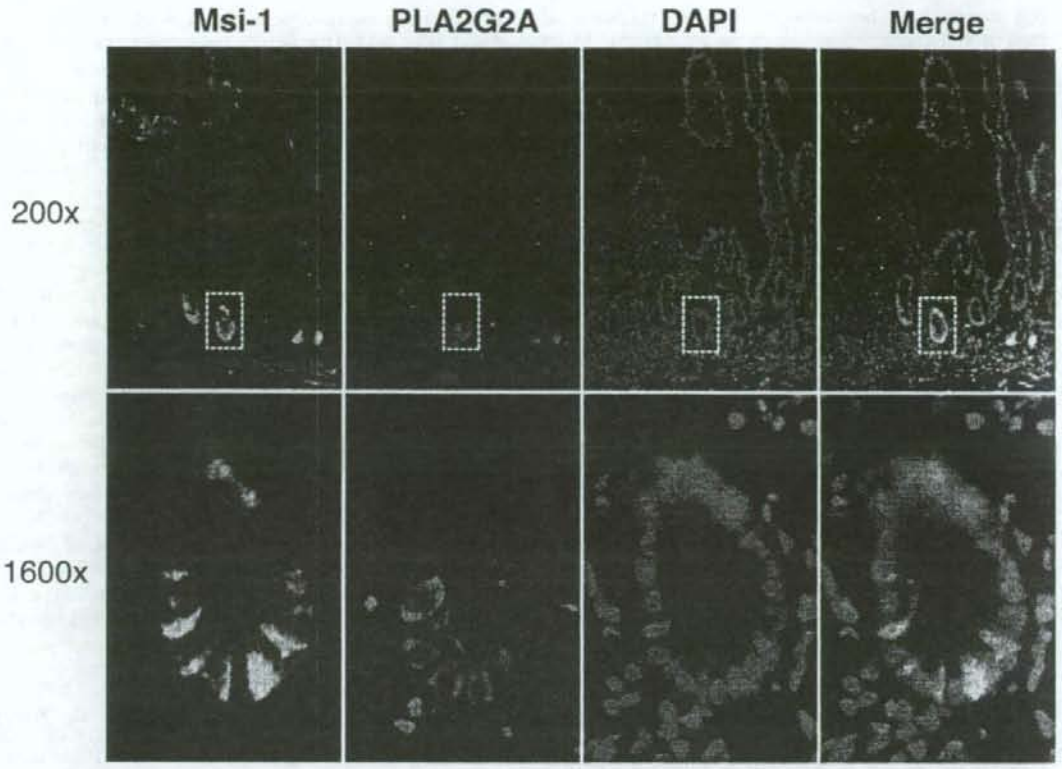

Fig. 5. Distinct cell population within the human intestinal crypt express Msi-1 or PLA2G2A. Double immunofluorescence staining of Msi-1 and PLA2G2A using a human small intestinal tissue is shown. Positive signals for both Msi-1 (*green*) and PLA2G2A (*red*) are observed in epithelial cells residing at the lowest part of the crypt (*upper panel*). A magnified view (*lower panel*) of the designated area (*white squares, upper panel*) shows positive staining of Msi-1 and PLA2G2A, each in distinct intestinal epithelial cells (IECs); coexpression of both proteins in a single IEC is not observed

Distinct populations of crypt epithelial cells expressed Msi-1 or PLA2G2A in the human intestine

To examine whether such a function of Msi-1 might be prevalent also in vivo, we examined the distribution of Msi-1- and PLA2G2A-expressing IECs within the human intestine. Double immunofluorescence staining using human small intestinal tissue showed both Msi-1- and PLA2G2A-expressing IECs locating at the lowest part of the crypt (Fig. 5, upper series). However, a magnified view showed a clear difference in the distribution of Msi-1- and PLA2G2A-expressing IECs, and not a single cell was found to coexpress both proteins (Fig. 5, lower series). Msi-1 expression appeared to be restricted to a population of IECs called the basal columnar cells, characterized by columnar morphology with a thin nucleus, which correspond to the cells recently determined to be definite ISCs.[6] In contrast, PLA2G2A expression was restricted to square cells with rich cytoplasm and a round nucleus, confirming its expression in mature Paneth cells. These findings show that although IECs expressing Msi-1 or PLA2G2A both clustered at the lowest part of the crypt, they each formed a distinct population of cells that were either extremely undifferentiated or fully mature, respectively. As this distribution of Msi-1 and PLA2G2A expression in the human intestine is fully consistent with our previous results, the result suggests that Msi-1 might function as a negative regulator of PLA2G2A expression also in vivo, and thereby contribute to maintain the undifferentiated state of ISCs.

Discussion

In the present study, we demonstrated that expression of Msi-1 in LS174T cells not only induced changes in

cell morphology but also suppressed expression of Paneth cell-specific genes such as *PLA2G2A*. Msi-1 appeared to downregulate *PLA2G2A* expression at the mRNA level by a molecular mechanism independent of the Notch- and Wnt- pathways. As we found that mature Paneth cells, residing adjacent to putative ISCs in vivo, completely lacked Msi-1 expression, loss of Msi-1 expression might be a key event during the process of Paneth cell differentiation from ISCs.

Although *Msi-1* has been reported to be a putative marker gene for ISCs, its functional importance has remained largely unknown.[8,9] As one of the common features of stem cells is to remain undifferentiated, suppression of IEC differentiation could be raised as one possible function of Msi-1. Consistent with this, our present study showed a significant decrease of Paneth cell-specific genes upon Msi-1 expression, suggesting that Msi-1 might function as a negative regulator for IEC differentiation. However, no effect was observed upon genes specific to other lineages, such as *MUC-2* (Fig. 2B). These results may further confirm that maintenance of undifferentiated state in ISCs requires involvement of multiple signaling pathways and molecules, including Msi-1.

Concerning the mechanism of Paneth cell differentiation, previous studies have shown that molecular pathways such as Wnt, Notch, and PPAR-β/δ play critical roles in the development of murine Paneth cells.[7,10,21-23] From our present study, however, the molecular mechanism by which Msi-1 suppresses Paneth cell maturation remains unclear, as it appeared to function independently from both the Notch and Wnt pathways. Further analysis of the Msi-1 target gene within IECs may elucidate the molecular function of Msi-1 in Paneth cell maturation.

The importance of the present finding in vivo may be found in the lowest part of the crypt, where two distinct populations of Wnt-activated IECs reside: ISCs and Paneth cells. Although both types of cell express target genes of the canonical Wnt pathway, they are clearly different in terms of differentiation, as one remains extremely undifferentiated while the other is fully mature. This difference may be, at least in part, mediated by expression of Msi-1, through its function of suppressing Paneth cell differentiation. Thus, our results suggest that expression of Msi-1 in Wnt-activated ISCs may be critically required to avoid progression of the differentiation program toward Paneth cells.

In contrast to IEC differentiation, a series of studies have previously described the role of Msi-1 on IEC proliferation. A recent study using gene knockdown of *Msi-1* in colon cancer cells investigated its role in promoting cell proliferation.[24] Also, another study has reported that p21/CIP1/WAF1 is one of the direct targets of Msi-1.[25] Our present study, however, failed to prove increased cell proliferation upon expression of Msi-1 (Fig. 2A). This failure may due to the aberrant activation of the Wnt pathway in LS174T cells, as this pathway is well known to function as a strong promoter of cell proliferation.[26] Although we were able to observe a two- to threefold increase of TOP-Luc activity upon Msi-1 expression, it appeared to have no significant effect on target genes of the canonical Wnt pathway, thus suggesting that the Wnt signaling pathway might be already fully activated, and no additional function could be achieved in LS174T cells.

Another surprising effect of Msi-1 expression was the significant change in cell morphology and colony formation (Fig. 1C). LS174T cells usually grow in an aggregated form and show a piled-up colony of cells. LS174T/Msi-1 cells, however, grew as a flat monolayer and never formed a colony of piled-up cells. These observations suggested that Msi-1 might also regulate arrangement of the cell cytoskeleton, thereby modulating cell–cell contact or cell motility. Such issues remain to be elucidated in future studies.

In conclusion, Msi-1 suppressed expression of Paneth cell-specific genes, including *PLA2G2A*, in IECs. These findings not only suggest that Msi-1 is a negative regulator of Paneth cell differentiation but also provide insight into functional aspects of Msi-1 expression within ISCs.

Acknowledgments. We express our thanks to Dr. Tetsuo Sudo, Dr. Ryoichiro Kageyama, and Dr. Hideyuki Okano for providing plasmids and antibodies, and to Dr. Hisao Fukushima and Dr. Kazutaka Koganei for providing tissue samples. This study was supported in part by Grants-in-Aid for Scientific Research, Scientific Research on Priority Areas, Exploratory Research, and Creative Scientific Research from the Japanese Ministry of Education, Culture, Sports, Science and Technology; the Japanese Ministry of Health, Labour and Welfare; the Japanese Society of Gastroenterology; the Foundation for Advancement of International Science; the Research Fund of Mitsukoshi Health and Welfare Foundation; and the Research Fund of Japan Intractable Diseases Research Foundation.

References

1. Bjerknes M, Cheng H. Gastrointestinal stem cells. II. Intestinal stem cells. Am J Physiol Gastrointest Liver Physiol 2005;289: G381–7.
2. Moore KA, Lemischka IR. Stem cells and their niches. Science 2006;311:1880–5.
3. Scoville DH, Sato T, He XC, Li L. Current view: intestinal stem cells and signaling. Gastroenterology 2008;134:849–64.
4. Nakamura T, Tsuchiya K, Watanabe M. Crosstalk between Wnt and Notch signaling in intestinal epithelial cell fate decision. J Gastroenterol 2007;42:705–10.
5. Crosnier C, Stamataki D, Lewis J. Organizing cell renewal in the intestine: stem cells, signals and combinatorial control. Nat Rev Genet 2006;7:349–59.

6. Barker N, van Es JH, Kuipers J, Kujala P, van den Born M, Cozijnsen M, et al. Identification of stem cells in small intestine and colon by marker gene *Lgr5*. Nature 2007;449:1003–7.
7. van Es JH, Jay P, Gregorieff A, van Gijn ME, Jonkheer S, Hatzis P, et al. Wnt signalling induces maturation of Paneth cells in intestinal crypts. Nat Cell Biol 2005;7:381–6.
8. Potten CS, Booth C, Tudor GL, Booth D, Brady G, Hurley P, et al. Identification of a putative intestinal stem cell and early lineage marker; musashi-1. Differentiation 2003;71:28–41.
9. Kayahara T, Sawada M, Takaishi S, Fukui H, Seno H, Fukuzawa H, et al. Candidate markers for stem and early progenitor cells, Musashi-1 and Hes1, are expressed in crypt base columnar cells of mouse small intestine. FEBS Lett 2003;535:131–5.
10. Imai T, Tokunaga A, Yoshida T, Hashimoto M, Mikoshiba K, Weinmaster G, et al. The neural RNA-binding protein Musashi1 translationally regulates mammalian numb gene expression by interacting with its mRNA. Mol Cell Biol 2001;21:3888–900.
11. Matsumoto T, Okamoto R, Yajima T, Mori T, Okamoto S, Ikeda Y, et al. Increase of bone marrow-derived secretory lineage epithelial cells during regeneration in the human intestine. Gastroenterology 2005;128:1851–67.
12. Okabe M, Imai T, Kurusu M, Hiromi Y, Okano H. Translational repression determines a neuronal potential in Drosophila asymmetric cell division. Nature 2001;411:94–8.
13. Okano H, Imai T, Okabe M. Musashi: a translational regulator of cell fate. J Cell Sci 2002;115:1355–9.
14. Oshima S, Nakamura T, Namiki S, Okada E, Tsuchiya K, Okamoto R, et al. Interferon regulatory factor 1 (IRF-1) and IRF-2 distinctively up-regulate gene expression and production of interleukin-7 in human intestinal epithelial cells. Mol Cell Biol 2004;24:6298–310.
15. Tsuchiya K, Nakamura T, Okamoto R, Kanai T, Watanabe M. Reciprocal targeting of Hath1 and beta-catenin by Wnt glycogen synthase kinase 3beta in human colon cancer. Gastroenterology 2007;132:208–20.
16. Aragaki M, Tsuchiya K, Okamoto R, Yoshioka S, Nakamura T, Sakamoto N, et al. Proteasomal degradation of Atoh1 by aberrant Wnt signaling maintains the undifferentiated state of colon cancer. Biochem Biophys Res Commun 2008;368:923–9.
17. Ayabe T, Ashida T, Kohgo Y, Kono T. The role of Paneth cells and their antimicrobial peptides in innate host defense. Trends Microbiol 2004;12:394–8.
18. Mori-Akiyama Y, van den Born M, van Es JH, Hamilton SR, Adams HP, Zhang J, et al. SOX9 is required for the differentiation of Paneth cells in the intestinal epithelium. Gastroenterology 2007;133:539–46.
19. Pinto D, Gregorieff A, Begthel H, Clevers H. Canonical Wnt signals are essential for homeostasis of the intestinal epithelium. Genes Dev 2003;17:1709–13.
20. Wang XY, Yin Y, Yuan H, Sakamaki T, Okano H, Glazer RI. Musashi1 modulates mammary progenitor cell expansion through proliferin-mediated activation of the Wnt and Notch pathways. Mol Cell Biol 2008;28:3589–99.
21. Yang Q, Bermingham NA, Finegold MJ, Zoghbi HY. Requirement of Math1 for secretory cell lineage commitment in the mouse intestine. Science 2001;294:2155–8.
22. Suzuki K, Fukui H, Kayahara T, Sawada M, Seno H, Hiai H, et al. Hes1-deficient mice show precocious differentiation of Paneth cells in the small intestine. Biochem Biophys Res Commun 2005;328:348–52.
23. Varnat F, Heggeler BB, Grisel P, Boucard N, Corthesy-Theulaz I, Wahli W, et al. PPARbeta/delta regulates paneth cell differentiation via controlling the hedgehog signaling pathway. Gastroenterology 2006;131:538–53.
24. Sureban S, May R, George R, Dieckgraefe B, Mcleod H, Ramalingam S, et al. Knockdown of RNA binding protein musashi-1 (Msi-1) leads to tumor regression in vivo. Gastroenterology 2008;134:1448–58.
25. Battelli C, Nikopoulos GN, Mitchell JG, Verdi JM. The RNA-binding protein Musashi-1 regulates neural development through the translational repression of p21WAF-1. Mol Cell Neurosci 2006;31:85–96.
26. van de Wetering M, Sancho E, Verweij C, de Lau W, Oving I, et al. The beta-catenin/TCF-4 complex imposes a crypt progenitor phenotype on colorectal cancer cells. Cell 2002;111:241–50.

Available online at www.sciencedirect.com
ScienceDirect
Biochemical and Biophysical Research Communications 368 (2008) 923–929
BBRC
www.elsevier.com/locate/ybbrc

Proteasomal degradation of Atoh1 by aberrant Wnt signaling maintains the undifferentiated state of colon cancer

Mikayo Aragaki [1], Kiichiro Tsuchiya [1], Ryuichi Okamoto, Sanae Yoshioka, Tetsuya Nakamura, Naoya Sakamoto, Takanori Kanai, Mamoru Watanabe *

Department of Gastroenterology and Hepatology, Graduate School, Tokyo Medical and Dental University, 1-5-45 Yushima, Bunkyo-ku, Tokyo 113-8519, Japan

Received 2 February 2008
Available online 12 February 2008

Abstract

Atoh1 plays a crucial role in intestinal cell differentiation. We have demonstrated that its human homolog Hath1 protein is targeted by the Wnt-GSK3 axis, resulting in the proteasomal degradation in human colon cancer. However, the contribution of Hath1 degradation to the undifferentiated state of colon cancer remains unknown. In this study, we demonstrated that both constitutive expression of mutant Hath1 and stabilization of Hath1 protein by a GSK3 inhibitor in colon cancer cells increased the expression of MUC2 known as a representative function of differentiated goblet cells. This means that Hath1 protein degradation may be required for maintaining the undifferentiated state of colon cancers, and that GSK3 inhibitors have potential for use in cancer therapy.

Keywords: Atoh1; Hath1; Proteasomal degradation; Differentiation; Wnt; GSK3β; Colon cancer

Atoh1 is a bHLH transcriptional factor that plays a critical role in terminal cell differentiation of intestinal epithelium, dorsal interneuron in the spinal cord, granule cells in the cerebellum, and inner hair cells in the auditory systems [1–4]. The mouse homolog of Atoh1, Math1, is expressed in the central nervous system and intestine in embryos but confined to the intestine in adults [5]. In Math1-deficient mice, loss of Math1 induces depletion of secretory cells such as Paneth cells, enteroendocrine cells and goblet cells, indicating that continuous expression of Atoh1 is required for proper differentiation and maintenance of epithelial homeostasis in intestine throughout the life span [4]. The human homolog of Atoh1, Hath1, is also strongly expressed in normal colon and small intestine [6,7], suggesting that it likewise contributes to the terminal differentiation of intestinal epithelial cells.

Dysregulation of Hath1 expression is thought to induce various diseases of the intestinal tracts. Loss of Hath1 protein has been observed in colorectal cancer, where Wnt signaling is constitutively activated by the truncated mutation of the adenomatous polyposis coli gene (APC); and Hath1 mRNA expression was found to be down-regulated in some colon cancer tissues compared with normal colon [6,7]. Thus, repression of Hath1 mRNA in colon cancer might promote maintenance of the undifferentiated state. However, not all colorectal cancers show low expression of Hath1 mRNA [6–8]. We have reported that Hath1 protein was lost in colorectal cancer even in the presence of Hath1 mRNA [7].

To clarify this anomaly in the expression of Hath1 protein and mRNA in colon cancer, we have examined the regulation of Hath1 protein stability in colon cancer-derived cell lines. Our previous study demonstrated that Hath1 protein was actively degraded by the ubiquitin–proteasome system via Wnt signaling that switched the target of

Abbreviations: APC, Adenomatous polyposis coli; GSK3β, glycogen synthase kinase 3β.

* Corresponding author. Fax: +81 3 5803 0262.
E-mail address: mamoru.gast@tmd.ac.jp (M. Watanabe).

[1] Both authors equally contributed to this work.

0006-291X/$ - see front matter © 2008 Elsevier Inc. All rights reserved.
doi:10.1016/j.bbrc.2008.02.011

GSK3β from β-catenin to Hath1 in colon cancer cells [7]. Aberrant Wnt signaling by truncated APC has been highlighted as the most critical trigger for carcinogenesis in colon, being observed in approximately 80% of patients with colorectal cancer [9,10]. Although it has been supposed that the accumulated β-catenin protein resulting from the aberrant Wnt signaling induced carcinogenesis and maintained the undifferentiated state of colon cancer, we have found that the Wnt signaling induced not only the continuous expression of β-catenin protein but also proteasomal degradation of Hath1 protein. Moreover, the inactivation of Wnt signaling by forced expression of the full-length APC gene in colon cancer cells gave rise to both β-catenin protein degradation and Hath1 protein stabilization, resulting in the cell differentiation toward goblet cells [7].

These results raise questions of whether is more effective in maintaining the undifferentiated state of colon cancer, uncontrolled expression of β-catenin or proteasomal degradation of Hath1, and whether the expression of Hath1 protein alone has the potential to promote the differentiation of intestinal epithelial cells even with β-catenin accumulation promoting the proliferating state.

In this study, we aimed to elucidate the effect of Hath1 protein stability on the undifferentiated state in human colon cancer. We found that the mutant Hath1 protein in which serine residues were replaced with alanine was stably expressed in human colon cancer cells with the aberrant Wnt signaling, resulting in the induction of differentiation toward goblet cells. We also demonstrated that treatment with a GSK3 inhibitor stabilized Hath1 protein and directed the colon cancer cells toward goblet cells, suggesting that GSK3 inhibitors have potential for use in a new therapeutic approach for the majority of patients suffering from colorectal cancers.

Materials and methods

DNA constructs. Expression plasmids used for this study were generated as reported previously [7].

Cell culture and creation of transient and stable cell lines. Human colon adenocarcinoma-derived SW480, DLD-1 cells, and human embryonic kidney-derived 293T cells were cultured in Dulbecco's modified Eagle's medium (Life Technologies, Grand Island, NY) supplemented with 10% fetal bovine serum and 1% penicillin–streptomycin. In all experiments 1×10^6 cells were grown in 6-cm dishes and were transiently transfected by using TransIT transfection reagent (Mirus, Madison, WI) according to the manufacturer's protocol with 4 μg of expression plasmids. Transfected cells were cultured under the usual conditions or in the presence of 10 μmol/L MG132 (Calbiochem) or 100 mmol/L LiCl (Sigma–Aldrich). Stable cell lines in DLD-1 were constructed with the Tet-On system with tet-repressor, pcDNA4-Flag Hath1 or Flag SA Hath1 plasmids. For selection, both blasticidin (7.5 μg/ml) and zeocin (750 μg/ml) were added for WT and SA cells. Hath1 gene expression was induced by cultivation in the presence of doxycycline for 12 h or more. After cultivation with doxycycline, MG132 (10 μmol/L) was added to the media and cultivation was continued for 8 h.

Western blot analysis. Cells were extracted with 1% sodium dodecyl sulfate (SDS)-containing radioimmunoprecipitation assay (RIPA) buffer as previously described [7]. The supernatants were removed and quantitated using protein assay reagent (Pierce, Rockford, IL). Preparations of 50 μg or 100 μg of proteins were separated in 12% SDS–polyacrylamide gels, transferred to polyvinylidene difluoride (PVDF) membranes according to standard procedures. The membranes were immunoblotted with anti-Flag M2 (Sigma Chemical Co., St. Louis, MO), anti-β-catenin (BD Biosciences Pharmingen), and anti-USF2 (Santa Cruz Biotechnology), then incubated with the secondary antibodies.

Luciferase assays. 293T cells were transiently transfected with 10 ng of *Renilla* luciferase reporter plasmid pRL-TK-Luc (Promega) along with 100 ng of either E-box-Luc or MUC2-Luc reporter plasmid and 100 ng of the expression plasmids. The data are represented as total relative light units (RLU) on histograms showing the average ± SEM of triplicate determinations.

Real-time PCR. SW480 cells were transiently transfected as indicated previously, then stimulated with 100 mmol/L LiCl for 8 h. DLD-1cells with the Tet-On system were stimulated with doxycycline for 5 d. Total RNA was isolated using TRIzol reagent (Invitrogen). Aliquots of 1 μg of total RNA were used for reverse transcription (Qiagen). Quantitative polymerase chain reaction was carried out using lightcycler (Roche) in triplicate to measure mRNA expression of Mucin2 (MUC2), Hath1, c-myc, and CDX2. The following Hath1 and CDX2 specific primers were used: Hath1 forward primer 5′-GCC CAA ATC TAC ATC AAC GCC-3′; Hath1 reverse primer 5′-TTG CCC GCG CCC CCT TCA TAG-3′; CDX2 forward primer 5′-CGG CTG GAG CTG GAG AAG G-3′; and CDX2 reverse primer 5′-TCA GCC TGG AAT TGC TCT GC-3′. Primers for MUC2 and c-myc were as described previously [7].

Immunocytochemistry. DLD-1 Tet-On cells were incubated in MG132 for 8 h following stimulation by doxycycline for 12 h, were fixed with 2.0% paraformaldehyde and were permeabilized with 0.5% Triton-X in PBS. Anti-Flag M2 antibody diluted with PBS was utilized to detect Flag-tagged Hath1. Incubation with anti-mouse IgG HRP-linked whole antibody (Amersham Biosciences) as the secondary antibody followed.

Results

A mutant Hath1 protein showed enhanced protein stability while maintaining its transcriptional activity in colon cancer cells

To determine the contribution of Hath1 protein stability to cell differentiation of colon cancer, we first attempted to express Hath1 protein stably in colon cancer cells. We have previously confirmed the protein stability of various mutant Hath1 constructs in colon cancer cells and found the critical region for Hath1 degradation to be the 54th and 58th serine residues of Hath1 protein [7]. The mutants represented in Fig. 1A were as follows. N1 and N5 are N-terminal deletion mutants of Hath1 preserving or excluding the critical serine residues, respectively. SA is a mutant in which the 54th and 58th serine residues are replaced with alanine residues (Fig. 1A). Wild-type (WT) and mutants of Hath1 transiently transfected into 293T cells with inactive Wnt signaling were confirmed to express all proteins stably (Fig. 1B). When transfected into the human colon cancer cell line with active Wnt signaling, both WT and N1 were degraded by the ubiquitin–proteasome system, while both N5 and SA were stably expressed even in the absence of the proteasome inhibitor MG132, as previously found (Fig. 1C). Although it has been reported that Hath1 binds to E-box sequences to activate the transcription of target genes [5], the critical region for the transcriptional activity of Hath1 remains unknown. We therefore per-

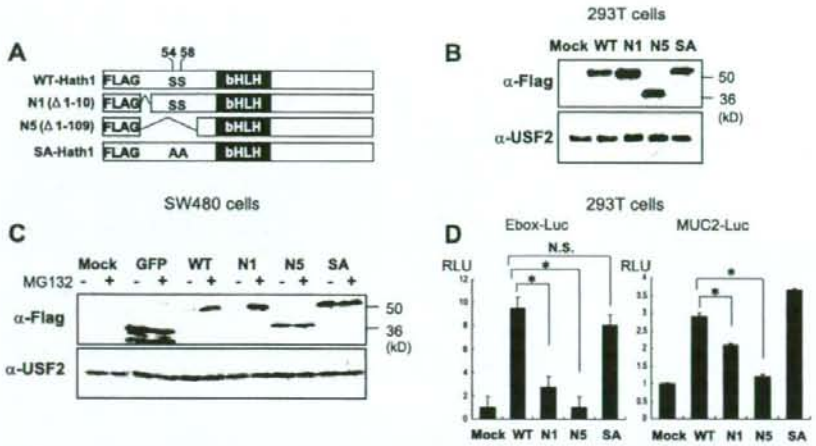

Fig. 1. Hath1 protein induced by alanine-substituted mutant showed enhanced stability while maintaining its transcriptional activity. (A) Schematic representation of various Flag-tagged Hath1 mutants used in this study. The N-terminal deleted regions of each mutant are designated by amino acid numbers. Serine residues at positions 54 (S54) and 58 (S58) are indicated. (B) 293T cells in which Wnt signaling is inactive were transfected with two of the N-terminal deletion mutants and a substituted mutant of Hath1 in addition to the WT. (C) SW480 cells were transfected by the same procedure as (B). WT and N1 mutant preserving the critical regions for protein degradation were detected only in the presence of MG132. N5 and SA lacking the critical regions expressed the proteins without the reagent. (D) 293T cells were co-transfected with of each of the WT and Hath1 mutants and either E-box Luc or MUC2 Luc. $^{*}P < 0.05$.

formed the luciferase assay with the Hath1 mutants in 293T cells (Fig. 1D). SA showed equivalent transcriptional activity to the wild-type, while N1 and N5 showed significantly reduced transcriptional activity, implying that the critical region for the transcriptional activity lies at the N-terminus of Hath1. Moreover, previous studies have noted a close association of Hath1 with MUC2 gene expression [6–8] and the transactivation of MUC2 promoter by Hath1 [8]. We found that SA and WT Hath1 showed equivalent transcriptional activity of MUC2, while N1 and N5 lost this activity (Fig. 1D).

Stable expression of SA Hath1 increases its transcriptional activity

Since only the SA mutant of Hath1 was stably expressed while maintaining its transcriptional activity in colon cancer cells, we considered that SA Hath1 was suitable to assess whether Hath1 has the potential to promote differentiation in colon cancer. We then constructed a cell line stably expressing the SA Hath1 protein through the Tet-On system in which expression of a target gene is induced by doxycycline. Expression of WT Hath1 protein was not induced by doxycycline alone, while SA was expressed regardless of treatment with MG132 (Fig. 2A). Moreover, immunofluorescence analysis revealed that SA Hath1 protein was expressed in the nucleus even in the absence of MG132 (Fig. 2B). Next, we examined the E-box-dependent transcriptional activity of SA Hath1 in colon cancer cells. Luciferase assay showed that the transcriptional activity of SA Hath1 is notably higher than of WT Hath1, possibly because of the increased amount of protein bound to E-box sequences (Fig. 2C).

Stable expression of SA Hath1 induces MUC2 mRNA on active Wnt signaling

Because the transcriptional activity of SA Hath1 was higher than of WT Hath1 in colon cancer cells, we further investigated whether constitutive Hath1 protein expression could induce differentiation characteristics in colon cancer cells. MUC2 mRNA expression was significantly up-regulated by the stable expression of SA Hath1 with doxycycline stimulation for 5 d, suggesting that SA Hath1 protein might induce the differentiated state of colon cancer cells (Fig. 3A). On the other hand, WT Hath1 was actively degraded by the proteasome system, resulting in the invariable expression of MUC2 mRNA. Next we examined whether MUC2 expression in colon cancer cells was related to the up-regulation of CDX2, since transcription of the MUC2 gene is reported to be induced by CDX2 binding to the MUC2 promoter [11]. Quantitative real-time RT-PCR assay revealed that CDX2 mRNA was not up-regulated, suggesting that MUC2 mRNA up-regulation by stable expression of Hath1 was independent of CDX2 in colon cancer cells (Fig. 3B). Importantly, Wnt signaling in SA Hath1 stable cell line is as active as in naive cells, because the amount of β-catenin and the expression of c-myc, which is one of the target genes of Wnt signaling, did not change in any of the cells (Fig. 3C and D). Together, these results indicate that stable Hath1 protein is itself sufficient to induce MUC2 mRNA without the

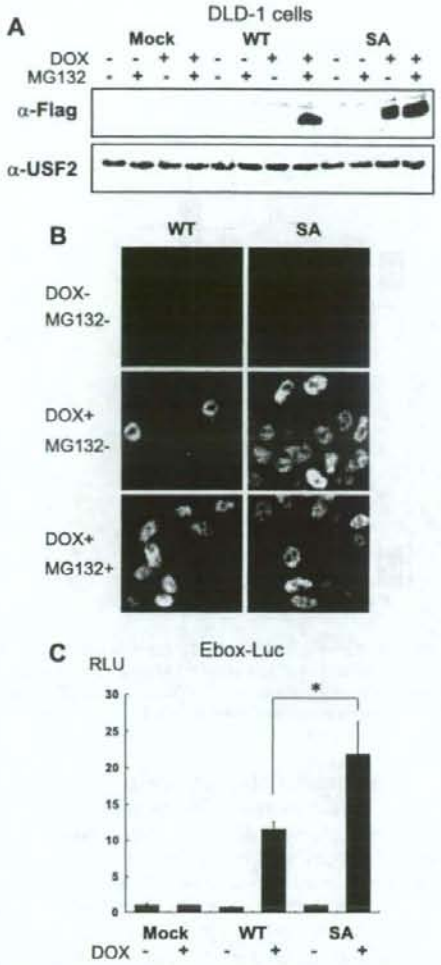

Fig. 2. DLD-1 stable cell line inducible for mutant SA Hath1 expression has increased transcriptional activity. (A) DLD-1 Tet-On cells were stimulated with doxycycline for 12 h before the incubation with MG132. (B) Immunocytochemical analysis of DLD-1 Tet-On cells in which expression from transfected SA Hath1 was performed to detect the SA Hath1 protein in the nucleus with or without MG132. (C) Luciferase assay was performed in DLD-1 Tet-On cells transfected with E-box Luc reporter plasmid. $^{*}P < 0.05$.

influence on constitutive expression of a group of target genes of β-catenin/TCF4 driving cell proliferation.

The GSK3 inhibitor stabilizes Hath1 protein, leading to up-regulation of MUC2 mRNA in colon cancer cells

As results suggested that SA Hath1 protein stably expressed in colon cancer cells was responsible for MUC2 mRNA expression, we investigated whether WT Hath1 stabilized by GSK3 inhibitors is able to induce MUC2 mRNA expression without the repression of Wnt signaling. Hath1 protein was detected in colon cancer cells incubated with a GSK3 inhibitor, LiCl, while the amount of β-catenin protein accumulated in the cells remained unchanged (Fig. 4A). Interestingly, WT Hath1 stabilized by LiCl increases MUC2 mRNA expression, suggesting that the stabilization of Hath1 protein is essential to induce definitive intestinal differentiation without the suppression of Wnt signaling in colon cancer cells (Fig. 4B).

Discussion

The results of this study demonstrate the significance of Hath1 protein stabilization in regulating the differentiation state of human colon cancer. We found that a Hath1 mutant in which serine residues were replaced with alanine (SA Hath1) is capable of stable expression while maintaining its transcriptional activity in colon cancer cells, and the N-terminus of Hath1 is essential for the E-box-dependent transcriptional activity. We demonstrated that the stable expression of SA Hath1 up-regulates its transcriptional activity, possibly through an increase in the amount of protein bound to E-box sequences. This results in increased expression of MUC2 mRNA, even in cells with accumulated β-catenin protein, which gives rise to the proliferated state. We further showed that the stabilization of WT Hath1 protein by a GSK3 inhibitor is adequate for the up-regulation of MUC2 mRNA in colon cancer cells, and propose that degradation of the Hath1 protein might lead to the undifferentiated state in colon cancer.

The significant role of Wnt signaling in healthy and malignant intestinal epithelium has been noted in terms of maintenance for both continuous proliferated and undifferentiated states [12,13]. Active Wnt signaling simultaneously promotes cell proliferation and inhibits differentiation through controlling c-myc and $p21^{CIP/WAF1}$ activity [13]. Our concern has been to find whether suppression of cell proliferation by inactivation of Wnt signaling leads exclusively the differentiated state in colon cancer. Focusing on the role of Hath1 in intestinal cell differentiation and its regulation at protein level, we contribute a new aspect to the establishment of neoplastic characteristics. Our findings in this study first suggest a partial contribution of Hath1 protein to the undifferentiated state in colon cancer. Hath1 protein degradation by active Wnt signaling might cause cell differentiation to halt, giving rise to the undifferentiated state viewed as one of characteristics of colon cancer. Our results are supported by the fact that, although Hath1 protein is expressed in only 7% of nonmucinous carcinomas, both Hath1 and MUC2 are expressed in more than 70% of mucinous cancers which have low malignant potential without APC deletion [8]. However, stabilization of Hath1 protein did not induce other differentiation markers such as phospholipase A2 (sPLA2), isomaltase and chromogranin A (CgA), in spite of the possibility of differentiation toward three secretory lineages

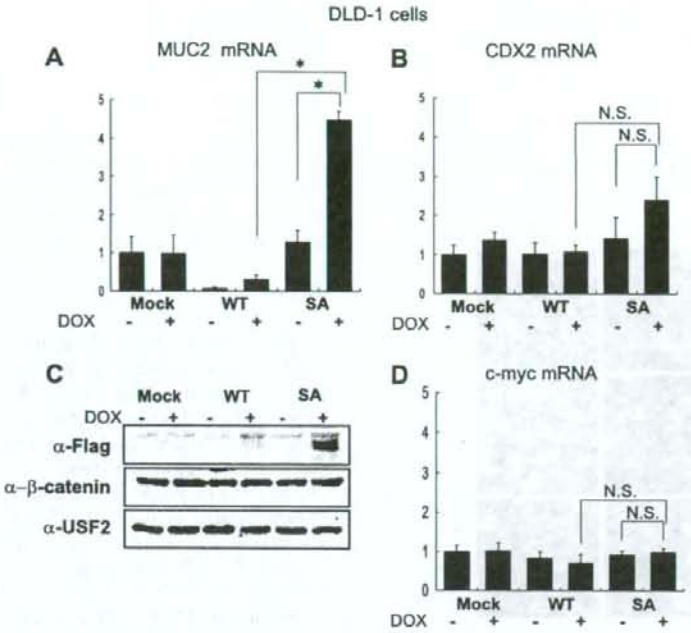

Fig. 3. Stabilization of Hath1 protein generates MUC2 mRNA independently of active Wnt signaling. (A) DLD-1 Tet-On cells were stimulated with doxycycline for 5 d. Results are expressed as the ratio of the levels of MUC2 mRNA to β-actin mRNA. $^{*}P < 0.05$. (B) (D) The same samples as in (A) were used to investigate CDX2 and c-myc mRNA expression, respectively. Results are expressed as the ratio of the levels of CDX2 and c-myc mRNA to β-actin mRNA. $^{*}P < 0.05$. (C) DLD-1 Tet-On cells were stimulated with doxycycline for 12 h. Immunoblotting was done with anti-β-catenin antibody.

(data not shown). The extent of the Hath1 contribution should be further analyzed.

Another important point of view in this study concerns the first phase of carcinogenesis. APC mutation has been revealed to promote the first stage initiation of carcinogenesis [14]. Immunohistochemical analysis of Hath1 protein expression in normal colon tissue by [6,7] suggests that APC mutation in colon cells might promote not only stable expression of β-catenin but also proteasomal degradation of Hath1 protein, leading to diminishment of Hath1 mRNA and resulting in the establishment of the undifferentiated state of cancer in the end stage. Therefore, in the early stage of carcinogenesis by APC deletion, the degradation of Hath1 protein is thought to be more essential than the diminishment of Hath1 mRNA in producing the undifferentiated state.

We finally propose that GSK3 inhibitors have potential for use in a new approach for anti-colon cancer drugs. Although many alternative therapies have been targeted to the Wnt signaling axis [15–17], development of a drug that targets Wnt signaling is difficult because of the complexity of the protein–protein interactions [15].

GSK3 is considered as a key enzyme in various neoplasms. Since many transcriptional factors, cell cycle regulators and proto-oncogenes act as substrates for GSK3, GSK3 has been considered as a suppressor of cellular neoplastic transformation [18]. Therefore, it has been suggested that GSK3 inhibitors might increase the risk of carcinogenesis [18,19]. LiCl, a relatively specific inhibitor of GSK3, has been used in therapies for bipolar disorder for many years, but the risk of cancer development in psychiatric patients treated with LiCl is even lower than in the general population, suggesting that LiCl may have a protective effect against cancer [20]. Another study indicates that the GSK3 inhibitors might not be sufficient to elevate the level of β-catenin protein in normal primary cells [21].

The benefits of GSK3 inhibitor use for colorectal cancer reduction have been described [22–24]. LiCl treatment in APC^{min} mouse does not increase the number of tumors compared with control, suggesting a low risk of cancer development [22]. Treatment with GSK3 inhibitors of mouse with subcutaneous xenografts of SW480 significantly inhibits proliferation of cancer cell xenografts, with no apparent pathological changes in other major organs [23]. Although, problematically, the molecular pathways and mechanisms involved in the anti-cancer effect of GSK3 inhibitors remain unclear [22–24], we have elucidated the molecular mechanisms of a GSK3 inhibitor in the reduction of colon cancer.

In conclusion, Hath1 protein has a potential to promote the differentiation of colon cancer cells independently of β-catenin accumulation, and stabilization of Hath1 protein

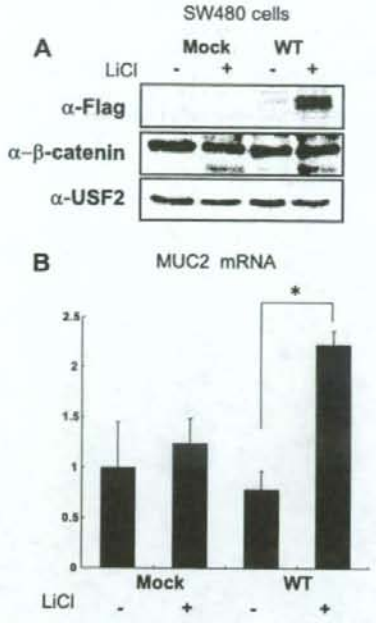

Fig. 4. The GSK3 inhibitor stabilizes Hath1 protein, leading to up-regulation of MUC2 mRNA in colon cancer cell lines. (A) SW480 cells were transiently transfected with WT Hath1 before 8 h of incubation in LiCl. Protein lysates were utilized for immunoblotting. (B) SW480 cells were transfected by the same procedure. Results of a quantitative real-time RT-PCR are expressed as the ratio of the levels of MUC2 mRNA to β-actin mRNA. $^{*}P < 0.05$.

by GSK3 inhibitors has intriguing therapeutic potential for colon cancer. Further detailed analyses of the switching mechanism of the GSK3β target between β-catenin and Hath1 on proteasomal degradation are required in order to introduce simple and pinpointed target therapies for colorectal cancers.

Acknowledgments

This work was supported in part by Grants-in-Aid for Scientific Research, and Creative Scientific Research on Priority Areas, Exploratory Research, and Creative Scientific Research from the Japanese Ministry of Education, Culture, Sports, Science, and Technology and the Japanese Ministry of Health, Labor, and Welfare.

References

[1] N. Ben-Arie, H.J. Bellen, D.L. Armstrong, A.E. McCall, P.R. Gordadze, Q. Guo, M.M. Matzuk, H.Y. Zoghbi, Math1 is essential for genesis of cerebellar granule neurons, Nature 390 (1997) 169–172.

[2] N.A. Bermingham, B.A. Hassan, S.D. Price, M.A. Vollrath, N. Ben-Arie, R.A. Eatock, H.J. Bellen, A. Lysakowski, H.Y. Zoghbi, Math1: an essential gene for the generation of inner ear hair cells, Science 284 (1999) 1837–1841.

[3] K. Gowan, A.W. Helms, T.L. Hunsaker, T. Collisson, P.J. Ebert, R. Odom, J.E. Johnson, Crossinhibitory activities of Ngn1 and Math1 allow specification of distinct dorsal interneurons, Neuron 31 (2001) 219–232.

[4] Q. Yang, N.A. Bermingham, M.J. Finegold, H.Y. Zoghbi, Requirement of Math1 for secretory cell lineage commitment in the mouse intestine, Science 294 (2001) 2155–2158.

[5] C. Akazawa, M. Ishibashi, C. Shimizu, S. Nakanishi, R. Kageyama, A mammalian helix-loop-helix factor structurally related to the product of *Drosophila* proneural gene atonal is a positive transcriptional regulator expressed in the developing nervous system, J. Biol. Chem. 270 (1995) 8730–8738.

[6] C.C. Leow, M.S. Romero, S. Ross, P. Polakis, W.Q. Gao, Hath1 down-regulated in colon adenocarcinomas, inhibits proliferation and tumorigenesis of colon cancer cells, Cancer Res. 64 (2004) 6050–6057.

[7] K. Tsuchiya, T. Nakamura, R. Okamoto, T. Kanai, M. Watanabe, Reciprocal targeting of Hath1 and beta-catenin by Wnt glycogen synthase kinase 3beta in human colon cancer, Gastroenterology 132 (2007) 208–220.

[8] E.T. Park, H.K. Oh, J.R. Gum Jr., S.C. Crawley, S. Kakar, J. Engel, C.C. Leow, W.Q. Gao, Y.S. Kim, HATH1 expression in mucinous cancers of the colorectum and related lesions, Clin. Cancer Res. 12 (2006) 5403–5410.

[9] P. Polakis, Wnt signaling and cancer, Genes Dev. 14 (2000) 1837–1851.

[10] P. Polakis, The oncogenic activation of beta-catenin, Curr. Opin. Genet. Dev. 9 (1999) 15–21.

[11] H. Yamamoto, Y.Q. Bai, Y. Yuasa, Homeodomain protein CDX2 regulates goblet-specific MUC2 gene expression, Biochem. Biophys. Res. Commun. 300 (2003) 813–818.

[12] D. Pinto, A. Gregorieff, H. Begthel, H. Clevers, Canonical Wnt signals are essential for homeostasis of the intestinal epithelium, Genes Dev. 17 (2003) 1709–1713.

[13] M. van de Wetering, E. Sancho, C. Verweij, W. de Lau, I. Oving, A. Hurlstone, K. van der Horn, E. Batlle, D. Coudreuse, A.P. Haramis, M. Tjon-Pon-Fong, P. Moerer, M. van den Born, G. Soete, S. Pals, M. Eilers, R. Medema, H. Clevers, The beta-catenin/TCF-4 complex imposes a crypt progenitor phenotype on colorectal cancer cells, Cell 111 (2002) 241–250.

[14] A.G. Renehan, S.T. O'Dwyer, N.J. Haboubi, C.S. Potten, Early cellular events in colorectal carcinogenesis, Colorectal Dis. 4 (2002) 76–89.

[15] J.H. van Es, M.E. van Gijn, O. Riccio, M. van den Born, M. Vooijs, H. Begthel, M. Cozijnsen, S. Robine, D.J. Winton, F. Radtke, H. Clevers, Notch/gamma-secretase inhibition turns proliferative cells in intestinal crypts and adenomas into goblet cells, Nature 435 (2005) 959–963.

[16] J.H. van Es, H. Clevers, Notch and Wnt inhibitors as potential new drugs for intestinal neoplastic disease, Trends Mol. Med. 11 (2005) 496–502.

[17] D.H. Palmer, M.J. Chen, D.J. Kerr, Gene therapy for colorectal cancer, Br. Med. Bull. 64 (2002) 201–225.

[18] P. Cohen, M. Goedert, GSK3 inhibitors: development and therapeutic potential, Nat. Rev. Drug Discov. 3 (2004) 479–487.

[19] A. Tighe, A. Ray-Sinha, O.D. Staples, S.S. Taylor, GSK-3 inhibitors induce chromosome instability, BMC Cell Biol. 8 (2007) 34.

[20] Y. Cohen, A. Chetrit, Y. Cohen, P. Sirota, B. Modan, Cancer morbidity in psychiatric patients: influence of lithium carbonate treatment, Med. Oncol. 15 (1998) 32–36.

[21] D.B. Ring, K.W. Johnson, E.J. Henriksen, J.M. Nuss, D. Goff, T.R. Kinnick, S.T. Ma, J.W. Reeder, I. Samuels, T. Slabiak, A.S. Wagman, M.E. Hammond, S.D. Harrison, Selective glycogen synthase kinase 3 inhibitors potentiate insulin activation of glucose transport and utilization in vitro and in vivo, Diabetes 52 (2003) 588–595.

[22] T.D. Gould, N.A. Gray, H.K. Manji, Effects of a glycogen synthase kinase-3 inhibitor, lithium, in adenomatous polyposis coli mutant mice, in adenomatous polyposis coli mutant mice, Pharmacol. Res. 48 (2003) 49–53.
[23] A. Shakoori, W. Mai, K. Miyashita, K. Yasumoto, Y. Takahashi, A. Ooi, K. Kawakami, T. Minamoto, Inhibition of GSK-3 beta activity attenuates proliferation of human colon cancer cells in rodents, Cancer Sci. 98 (2007) 1388–1393.
[24] J. Tan, L. Zhuang, H.S. Leong, N.G. Iyer, E.T. Liu, Q. Yu, Pharmacologic modulation of glycogen synthase kinase-3beta promotes p53-dependent apoptosis through a direct Bax-mediated mitochondrial pathway in colorectal cancer cells, Cancer Res. 65 (2005) 9012–9020.

Negative Feedback Regulation of Colitogenic CD4$^+$ T Cells by Increased Granulopoiesis

Yasuhiro Nemoto, MD, PhD, Takanori Kanai, MD, PhD,* Shuji Tohda, MD, PhD,† Teruji Totsuka, MD, PhD,* Ryuichi Okamoto, MD, PhD,* Kiichiro Tsuchiya, MD, PhD,* Tetsuya Nakamura, MD, PhD,* Naoya Sakamoto, MD, PhD,* Tetsuya Fukuda, MD, PhD,‡ Osamu Miura, MD, PhD,‡ Hideo Yagita, PhD,§ and Mamoru Watanabe, MD, PhD**

Background: Chronic inflammatory diseases are characterized by massive infiltration of innate and acquired immune cells in inflammatory sites. However, it remains unclear how these cells cooperate in the development of disease. Although bone marrow (BM) is a primary site for hematopoiesis of immune cells except T cells, BM recruits memory T cells from the periphery. We have recently demonstrated that colitogenic CD4$^+$ memory T cells reside in BM of colitic CD4$^+$CD45RB^{high} T-cell-transferred SCID mice. Based on this background we here investigate whether granulocytes promote or suppress the expansion of colitogenic CD4$^+$ T cells.

Methods: First, we show that Gr-1^{high}CD11b$^+$ granulocytes were significantly increased in colitic BM along with a significant increase of peripheral granulocytes. Consistently, the colony-forming unit (CFU) assay revealed that granulocyte colony formation was dominantly induced by supernatants from anti-CD3-stimulated colitic BM CD4$^+$ T cells.

Results: Administration of granulocyte-depleting anti-Gr-1 mAb to colitic mice did not ameliorate the colitis, but exacerbated the wasting disease with an increased expansion of systemic, but not lamina propria, CD4$^+$ T cells with activated phenotype.

Conclusions: These results suggest that the increased granulopoiesis by colitogenic BM CD4$^+$ T cells represent a negative feedback mechanism to control systemic inflammation.

(Inflamm Bowel Dis 2008;14:1491–1503)

Key Words: CD4$^+$ T cells, bone marrow, granulocytes, immune regulation, immunopathology

Inflammatory bowel diseases (IBDs) are caused by excessive tissue damage by chronic inflammatory responses in the gut wall and commonly take persistent courses.[1,2] According to our current understanding the diseases are caused by activated macrophages and effector CD4$^+$ T cells infiltrated in inflamed mucosa, which are presumably primed by commensal bacterial antigen-presenting dendritic cells in lymphoid tissues, such as mesenteric lymph nodes and Payer's patches.[3–8] Thus, recent studies mainly focus on lymphocytes, macrophages, and dendritic cells in addition to epithelial cells for the pathogenesis of IBD. Granulocytes are thought to be the first emerging cells in inflamed mucosa of human IBD in response to danger signals, such as epithelial damage, before the establishment of antigen-specific T-cell-mediated immune responses.[9–12]

Clinicopathologically, however, it is well known that abundant granulocytes are observed in inflamed mucosa of active IBD patients, and the degree of infiltrated granulocytes/neutrophils is a criteria for disease severity in the pathological scoring systems of both Crohn's disease and ulcerative colitis.[13] In addition, it has also been reported that the circulating activated granulocytes are elevated with increased survival time in patients with severe IBD.[14,15] Thus, we investigated the role of granulocytes in the pathogenesis of the chronic phase of colitis using a murine T-cell-mediated model of colitis induced by adoptive transfer of CD4$^+$CD45RB^{high} T cells into immunodeficient SCID mice.[16,17]

MATERIALS AND METHODS

Mice

BALB/c and C.B-17 SCID mice were purchased from Japan Clear (Tokyo, Japan). Mice were maintained under

Received for publication February 20, 2008; Accepted May 12, 2008.

From the *Department of Gastroenterology and Hepatology, †Department of Laboratory Medicine, ‡Department of Hematology, Graduate School of Medicine, Tokyo Medical and Dental University, §Department of Immunology, Juntendo University School of Medicine, Tokyo, Japan.

Supported in part by grants-in-aid for Scientific Research, Scientific Research on Priority Areas, Exploratory Research and Creative Scientific Research from the Japanese Ministry of Education, Culture, Sports, Science and Technology; the Japanese Ministry of Health, Labor and Welfare; the Japan Medical Association; Foundation for Advancement of International Science; Terumo Life Science Foundation; Ohyama Health Foundation; Yakult Bio-Science Foundation; Research Fund of Mitsukoshi Health and Welfare Foundation.

Reprints and current address: Takanori Kanai, MD, Division of Gastroenterology and Hepatology, Department of Internal Medicine, Keio University School of Medicine, T, 35 Sinanomachi, Shinjuku-ku, Tokyo 160-8582, Japan (e-mail: takagast@sc.itc.keio.ac.jp).

DOI 10.1002/ibd.20531

Published online 11 July 2008 in Wiley InterScience (www.interscience.wiley.com).

specific pathogen-free (SPF) conditions in the Animal Care Facility of Tokyo Medical and Dental University. Donors and littermate recipients were used at 6–12 weeks of age. All experiments were approved by the regional animal study committees and were done according to institutional guidelines and Home Office regulations.

Antibodies

The following mAbs other than purified antimouse Gr-1 mAb (RB6-8C5), biotin-conjugated antimouse IL-7Rα (A7R34; eBioscience, San Diego, CA), PE-conjugated antimouse CD11b (M1/70; eBioscience), and PE-conjugated anti-F4/80 (CI:A3-1; Serotec, Bicester, UK) were obtained from BD Pharmingen (San Diego, CA) and used for purification of cell populations and flow cytometric analysis: FcγR (CD16/CD32)-blocking mAb (2.4G2), FITC-, PE-, PECy5-, PerCP-, or APC-conjugated antimouse CD4 (RM4-5); FITC- or PerCP-conjugated antimouse CD3 (145-2C11); FITC-conjugated antimouse CD45RB (16A); FITC-conjugated antimouse CD62L (MEL-14); FITC-conjugated antimouse CD69 (H1.2F3); FITC-conjugated antimouse Gr-1 (RB6-8C5); FITC-conjugated antimouse CD11c (7D4); PE-conjugated anti-Ly6G (1A8); biotin-conjugated anti-Ly6C (AL-21); PE-conjugated anti-CD31 (MEC13.3); biotin-conjugated rat IgG2; PE-conjugated mouse IgG; and PE-conjugated rat IgG.

Induction of Colitis

Colitis was induced in SCID mice by adoptive transfer of $CD4^+CD45RB^{high}$ T cells (17). Briefly, $CD4^+$ T cells were isolated from splenocytes using the anti-CD4 (L3T4) MACS magnetic separation system (Miltenyi Biotec, Auburn, CA). Enriched $CD4^+$ T cells were labeled with PE-conjugated antimouse CD4 mAb and FITC-conjugated anti-CD45RB mAb, then sorted to yield the $CD45RB^{high}$ (highest staining 30%) fraction on a FACS Vantage SE (Becton Dickinson, Sunnyvale, CA). Each SCID mouse was injected intraperitoneally with 3×10^5 $CD4^+CD45RB^{high}$ T cells. The colitic mice induced by the adoptive transfer of $CD4^+CD45RB^{high}$ T cells were sacrificed at 6–8 weeks after transfer.

T-cell Preparation

For isolation of peripheral lymphocytes, 600 μL of peripheral blood was collected from each mouse and diluted 1:1 with phosphate-buffered saline (PBS). The diluted blood was layered over Lymphosepar II (IBL, Gunma, Japan) and centrifuged at 400*g* for 20 minutes at room temperature. Spleen (SP) was mechanically disrupted into single cell suspensions. BM was collected from the femur by flushing with sterile PBS. To assess cells for the preparation of colonic LP cells,[18] colon was first flushed extensively to eliminate the lumen content, then longitudinally opened and cut into small pieces. The dissected mucosa was incubated with Ca++ Mg++-free Hank's BSS containing 1 mM DTT (Sigma-Aldrich, St. Louis, MO) for 30 minutes to remove mucus, then treated with 1 mg/mL collagenase (Worthington Biomedical, Freehold, NJ) and 0.01% DNase (Worthington) for 2 hours. After filtering through gauze, cells were pelleted twice through a 40% isotonic Percoll solution and then subjected to Ficoll-Hypaque density gradient centrifugation (40%/75%). Enriched $CD4^+$ T cells were obtained by positive selection using anti-CD4 (L3T4) MACS magnetic beads. The resultant cells contained >94% $CD4^+$ cells when analyzed by FACS Calibur.

Flow Cytometry

To detect the surface expression of a variety of molecules, isolated cells were preincubated with the FcγR-blocking mAb for 20 minutes followed by incubation with specific FITC-, PE-, PerCP-, APC-, or biotin-labeled antibodies for 30 minutes on ice. Biotinylated antibodies were detected with PE-streptavidin. Standard 2-, 3-, or 4-color flow cytometric analyses performed on FACS Calibur and CellQuest software. Background fluorescence was assessed by staining with control isotype-matched mAbs.

Cytokine ELISA

To measure cytokine production, 1×10^5 $CD4^+$ T cells from LP and BM were cultured in 200 μL of culture medium at 37°C in a humidified atmosphere containing 5% CO_2 in 96-well plates (Costar, Cambridge, MA) precoated with 5 μg/mL hamster antimouse CD3e mAb (145-2C11, BD Pharmingen) and 2 μg/mL hamster antimouse CD28 mAb (37.51, BD Pharmingen) in PBS overnight at 4°C. Culture supernatants were removed after 48 hours and assayed for cytokine production. Cytokine concentrations were determined by specific ELISA as per the manufacturer's recommendation (R&D, Minneapolis, MN).

Immunohistochemistry

Consecutive cryostat bone marrow sections (6 μm) were fixed and stained with the following rat antibodies by a 4-step method. First, the sections were stained with purified anti-Gr-1 antibodies (RB6-8C5), followed by staining with Alexa 594 goat antirat IgG (Molecular Probes, Eugene, OR). The sections were then stained with biotinylated anti-CD4 (RM4-5; BD Pharmingen), following by staining with Alexa 488 streptavidin (Molecular Probes). All confocal microscopy was carried out on a BioZERO BZ8000 (Keyence, Tokyo).

Colony-forming Unit (CFU) Assay

Unseparated femoral BM from wildtype BALB/c mice were plated at 5×10^5 cells/mL in MethoCult without cytokines (Stem Cell Technologies, Vancouver, BC, Canada) in the presence of 2000-fold diluted supernatants obtained from

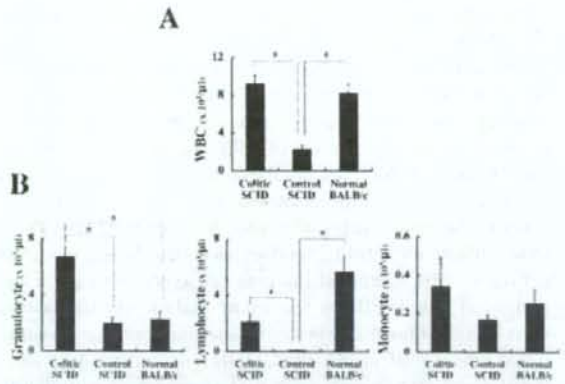

FIGURE 1. Neutrophils are markedly increased in peripheral blood of mice with established chronic colitis. A: WBC counts in colitic SCID mice 6 weeks after transfer, age-matched control SCID mice, and normal BALB/c mice. B: Cell counts of different compartments in colitic SCID mice 6 weeks after transfer, age-matched control SCID mice and normal BALB/c mice were determined by flow cytometry. Error bar indicates SEM for 10 mice of each group. $^*P < 0.05$.

anti-CD3/CD28 mAbs-stimulated colitic or normal BM or LP $CD4^+$ T cells for 48 hours. Colonies were scored 7 days after incubation of cells at 5% CO_2 in a humidified atmosphere.

In Vivo Experimental Design

We first checked whether in vivo anti-Gr-1 treatment preferentially depletes granulocytes, but not dendritic cells and macrophages, and myeloid suppressor cells by assessing the expression of Ly-6G molecule that is a more specific marker for granulocytes, CD11c, F4/80, and CD31 in addition to CD11b and Gr-1 on cells obtained from various sites of colitic mice administered anti-Gr-1 mAb (250 μg) or control IgG (250 μg) every 8 hours 3 times for 1 day before sacrifice. Then the expression of F4/80 (macrophage marker), CD11c (dendritic cell), and CD31 (myeloid suppressor cells)[19] on $CD11b^+Gr\text{-}1^{high}$ or $CD11b^+Gr\text{-}1^{low}$ cells was examined using flow cytometry. As a long-term administration of anti-Gr-1 mAb, each SCID mouse was injected i.p. with 200 μL of PBS containing 3×10^5 $CD4^+CD45RB^{high}$ T cells. These mice were then i.p. administered 250 μg of anti-Gr-1 mAb in 250 μL PBS 3 times per week, starting at the day of transfer or at 3 weeks after T-cell transfer. An equivalent amount of control rat IgG (Sigma) was administered in positive control mice. Negative control SCID mice were transferred with a mixture of 3×10^5 $CD4^+CD45RB^{high}$ and 3×10^5 $CD4^+CD45RB^{low}$ T cells. In another set of in vivo experiments, SPX SCID mice were used as recipient mice to exclude a possible contribution of the spleen to granulopoiesis in this model.

The recipient mice after transfer were weighed initially, then 3 times per week thereafter. They were observed for clinical signs of illness: hunched over appearance, piloerection of the coat, diarrhea, and blood in the stool. Mice were sacrificed at the indicated timepoint and assessed for a clinical score that is the sum (0–8 points) of 4 parameters as follows: hunching and wasting, 0 or 1; colon thickening, 0–3 (0, no colon thickening; 1, mild thickening; 2, moderate thickening; 3, extensive thickening); stool consistency, 0–3 (0, normal beaded stool; 1, soft stool; 2, diarrhea); and an additional point was added if gross blood was noted.[20] To monitor the clinical signs during the observed period over time, the disease activity index is defined as the sum (0–5 points) of the above-mentioned parameters except colon thickening. To assess the histological scores, tissue samples were fixed in PBS containing 6% neutral-buffered formalin. Paraffin-embedded sections (5 μm) were stained with hematoxylin and eosin (H&E). The sections were analyzed without prior knowledge of the type of T-cell reconstitution and recipients. The area most affected was graded by the number and severity of lesions. The mean degree of inflammation in

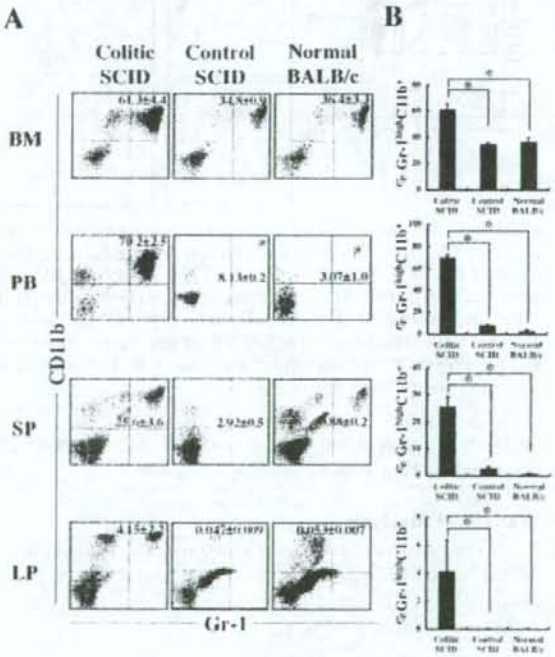

FIGURE 2. Granulocytes in colitic BM are markedly increased. A: BM, PB, SP, and LP cells of colitic SCID mice 6 weeks after transfer, age-matched control SCID mice, and normal BALB/c mice were analyzed by FACS for the expression of Gr-1 and CD11b cell-surface markers. B: Percentages of $Gr\text{-}1^{high}CD11b^+$ mature granulocytes. Error bar indicates SEM for 10 mice of each group. $^*P < 0.05$.

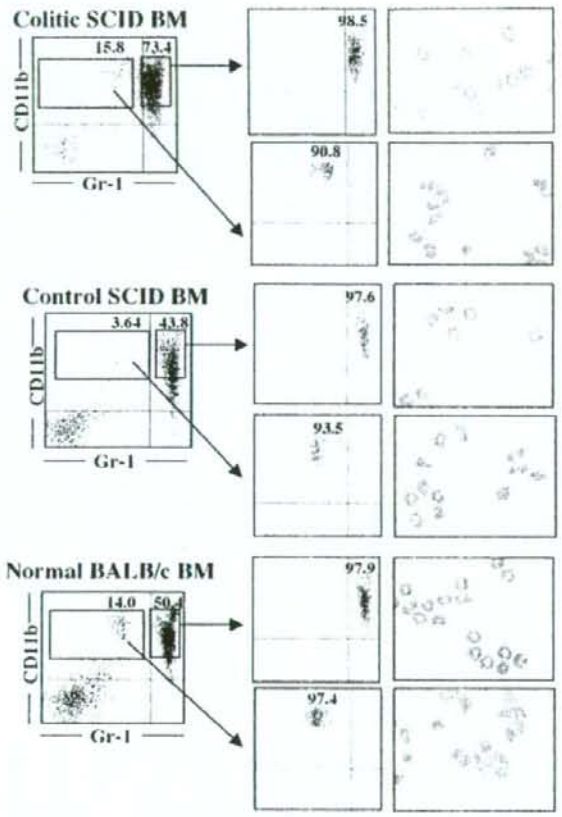

FIGURE 3. BM Gr-1^{high}CD11b^{+} cells are morphologically granulocytes. Cytospins staining with Wright was performed using isolated BM Gr-1^{high}CD11b^{+} and Gr-1^{low}CD11b cells. BM cells were isolated from colitic SCID mice, age-matched normal SCID mice, and normal BALB/c mice. Then Gr-1^{high}CD11b^{+} and Gr-1^{low}CD11b cells isolated using FACS Vantage were stained with Wright after cytospin procedures. Original, ×40. Data represent 3 independent experiments.

the colon was calculated using a modification of a previously described scoring system.[19]

Statistical Analysis

The results are expressed as the mean ± standard error of the mean (SEM). Groups of data were compared by Mann–Whitney *U*-test. Differences were considered statistically significant at $P < 0.05$.

RESULTS

Peripheral Granulocytes Are Markedly Increased in Mice with Chronic Colitis

Although SCID-transfer model of colitis induced by adoptive transfer of CD4^{+}CD45RB^{high} T cells is one of the representative CD4^{+} T-cell-mediated colitis models accompanied by the activation of antigen-presenting cells and CD4^{+} T cells,[3,16] the role of granulocytes in this model is largely unknown. Since it is generally believed that granulocytes are the early emerging innate immune cells that are involved in the acute phase of colitis in an antigen-nonspecific manner before the establishment of T-cell-mediated immune responses, little is known about the role of granulocytes in this model especially after developing colitis. Thus, to investigate the role of granulocytes in this chronic model of colitis we first examined immune cell compartments in the peripheral blood (PB) by a conventional blood examination of cell compartment. Expectedly, the total number of white blood cells (WBCs) in colitic SCID mice at 6 weeks after transfer was significantly increased as compared with that in nontransferred age-matched SCID (control SCID) and was comparable to that in normal BALB/c mice (Fig. 1A). Surprisingly, however, the major compartment of the increased peripheral WBC in colitic SCID mice was predominantly the granulocyte population rather than the lymphocyte population (Fig. 1B, left). In contrast, the number of lymphocytes in colitic mice was indeed significantly increased as compared with that in control SCID mice, but was significantly lower than that in normal BALB/c mice (Fig. 1B, middle). In addition, no significant differences in the numbers of monocytes among the 3 groups were observed (Fig. 1B, right).

BM Granulocytes Are Markedly Increased in Mice With Chronic Colitis

Given that peripheral granulocytes were significantly increased even after the chronic phase (6 weeks after transfer) of the T-cell-mediated colitis, we next assessed the granulocytes in various sites 6 weeks after transfer using flow cytometry. Interestingly, we found that the proportion of CD11b^{+}Gr-1^{high} granulocytes was significantly increased not only in PB, SP, and LP, but also in BM in colitic mice as compared with age-matched control SCID mice or normal BALB/c mice (Fig. 2A,B). We further confirmed that the population of CD11b^{+}Gr-1^{high} cells was morphologically categorized as granulocyte by showing that almost all the isolating BM CD11b^{+}Gr-1^{high} cells from colitic SCID, control SCID, and normal BALB/c mice were preferentially polymorphonuclear-shaped (Fig. 3), while isolated BM CD11b^{+}Gr-1^{low} cells from 3 groups of mice were a mixture of mononuclear and polynuclear cells (Fig. 3), suggesting that the increase of CD11b^{+}Gr-1^{high} granulopoiesis stimulated by the infiltrating colitogenic CD4^{+} T cells in BM is a cause of the systemic increase of granulocytes in colitic mice.

To further assess the association between increased numbers of granulocytes and CD4^{+} T cells in various sites of colitic mice, we assessed the numbers of CD11b^{+}Gr-1^{high} granulocytes and CD3^{+}CD4^{+} T cells in various sites at 4 and 10 weeks after transfer. During this course the clinical score